CDF/PUB/EXOTIC/PUBLIC/9160

High-Mass Dielectron Resonance Search in $p\bar{p}$ Collisions at $\sqrt{s}$ =1.96 TeV

The CDF Collaboration
URL http://www-cdf.fnal.gov
(Dated: March 6, 2008)

Based on 2.5 fb^{-1} of $p\bar{p}$ collision data collected with the CDF II detector at the Fermilab Tevatron at $\sqrt{s}$ =1.96 TeV, we report on a search for high-mass resonances in the dielectron channel. The most significant region of excess of data over background occurs for a dielectron invariant mass window of 240 GeV/c^2, and is 3.8 standard deviations above the Standard Model (SM) prediction. The probability of observing a background fluctuation with significance $(S/\sigma_B) \geq 3.8$ anywhere in the mass range of 150-1,000 GeV/c^2 is about 0.6%. The upper limits on $\sigma \cdot \Gamma(X \rightarrow ee)$ at 95% C.L. are set as a function of mass, where the Xs are spin-1 or spin-2 particles. The limits are translated to the mass limits with the SM coupling Z' and E_6 Z's for spin-1 particles and the Randall-Sundrum (RS) gravitons for spin-2 particles. The SM coupling Z' and the RS graviton with $k/\overline{M}_{Pl} = 0.1$ are excluded for masses below 966 and 850 GeV/c^2, respectively.

I. INTRODUCTION

The lepton-antilepton pair, in particular e^+e^- and $\mu^+\mu^-$, signature has been a leading discovery channel for new particles, such as J/ψ and Υ mesons, and the Z boson. Even though leptonic decay rates are generally lower than hadronic decay rates, these channels are preferred for particle searches since leptonic channels have relatively low backgrounds compared to hadronic channels. Furthermore, leptons are relatively easy to identify and their energies and momenta can be measured more precisely than hadrons.

Many models beyond the SM predict the existence of new particles decaying to lepton-antilepton pairs. The E_6 Z's [1] and the RS graviton [2] are the specific new particles decaying to a lepton-antilepton final state. The E_6 model predicts two additional neutral massive spin-1 bosons, referred to as Z's of which states are not mass eigen states. Six mass eigen states, Z'_ψ, Z'_χ, Z'_η, Z'_I, Z'_{sq} and Z'_N are built with specific mixing angles, which are used to examine the model. The RS graviton is the lightest neutral spin-2 particle predicted by the RS model which predicts a series of neutral spin-2 resonances. The RS model is examined with the parameter $k/\overline{M}_{Pl}$ which determines the couplings between the RS graviton and SM particles, where k is the negative curvature and $\overline{M}_{Pl}$ is the reduced effective Planck scale. The $k/\overline{M}_{Pl}$ is examined with a typical range of 0.01 to 0.1 [3].

In a recent publication, the CDF collaboration has set limits on the models by analyzing the dielectron invariant mass distribution of dielectron events with 1.3 fb^{-1} of integrated luminosity [4]. The lower mass limits for new particles vary from 302 to 923 GeV/c^2, depending on the models. This note describes a search for dielectron resonances over SM prediction in an invariant mass range of 150-1,000 GeV/c^2 with 2.5 fb^{-1} of data. The upper limits on $\sigma \times \Gamma(X \to ee)$ at 95% C.L. are also set, where the Xs are spin-1 or spin-2 particles. The lower bounds on masses of E_6 Z's and the RS graviton are set with the limits.

II. DATA SAMPLE & EVENT SELECTION

This analysis is based on an integrated luminosity of 2.5 fb^{-1} collected with the CDF II detector between March 2002 and August 2007. The CDF detector is described in detail in [5]. Three triggers are used to select the data for this analysis. The first trigger requires two EM clusters with E_T >18 GeV in the calorimeter, the second one requires a central EM cluster with E_T >70 GeV and the last one requires one central EM cluster with E_T >18 GeV and loose electron (throughout this note the charge conjugate state is implied) selection. For the latter two triggers, a well-measured track pointing to an energy deposition in the calorimeter is required. With these three triggers, the efficiency for events passing offline selections is ≈100%. For this analysis, we require an event to have one electron in the central region and the other electron in either the central or forward ("plug") region. The transverse energy of electrons is required to be greater than 25 GeV and the pseudo-rapidity of electrons is required to be within ±2. The central region electrons are required to have a well-measured track pointing at an energy deposition in the calorimeter. For electrons in the plug region, the track association uses a calorimeter-seeded silicon tracking algorithm [6].

III. BACKGROUNDS

There are three categories of background contributing to the dielectron final state. One is Drell-Yan (DY) production, which is the dominant source of background and is irreducible. Another is the QCD jet production in dijets and W+jets ("QCD"), where the jets are misidentified as electrons. Other than DY and QCD production, there are contributions from, $Z/\gamma^* \to \tau\tau$, $t\bar{t}$ and diboson ($W\gamma/WW/WZ/ZZ/\gamma\gamma$) production, which are referred to as "Other SM" backgrounds.

The DY Monte Carlo (MC) generated with PYTHIA [7] is used to estimate the DY contribution. The DY MC is normalized to the data in an invariant mass window from 76 to 106 GeV/c^2 for central-central (CC) dielectron events and from 81 to 101 GeV/c^2 for central-plug (CP) region events. The mass windows are different because the QCD background in the CP region events is higher than in the CC region. We assign 3.6% systematic uncertainty in the DY prediction due to the invariant mass dependency of the k-factor [8].

The QCD background estimation is data driven and is obtained using the probability for a jet to be misidentified as an electron ("fake rate"), which is measured with jet triggered data samples. The fake rate obtained from jet data is applied to each jet in events with one good electron candidate and one or more jets. Both W and Z boson events are removed from the sample before applying the fake rate for dijet background contribution. To estimate W+jet background, Z boson events are removed and W boson events are retained before applying the fake rate. The dominant systematic uncertainty on the QCD background is due to the fake rate uncertainty, which is 20%.

Other SM contributions are estimated with MC samples which are generated with PYTHIA except for the $W\gamma$ process. The $W\gamma$ is generated with the matrix element generator `WGAMMA` [9]. Other SM MC samples are normalized with

the theoretical cross sections and the total integrated luminosity. The dominant sources of systematic uncertainties for other SM background are from luminosity [10] (6%) and theoretical cross sections (8%).

IV. RESULTS

Fig. 1 shows the observed dielectron invariant mass spectrum from 2.5 fb^{-1} of data together with the expected total SM backgrounds described in Sec. III.

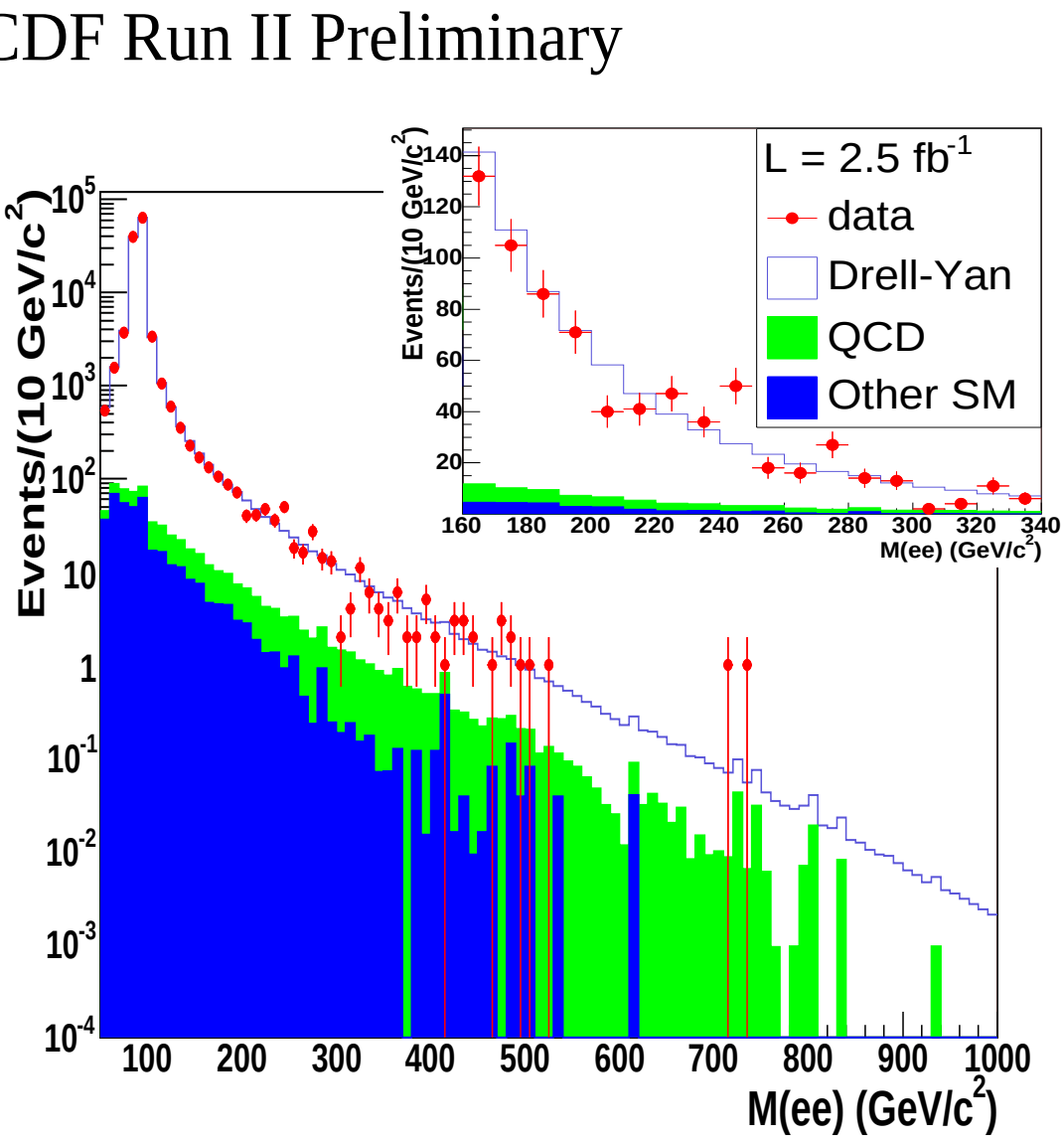

FIG. 1: Invariant mass distribution of dielectron data compared to the expected backgrounds, shown on a log scale. Red dots with error bars are data. The blue shaded region is "Other SM" background, the green region is "QCD" background, and the white region is $Z/\gamma^* \to e^+e^-$ background. The inset shows the same for the 240 GeV/c^2 region using a linear scale.

The search for resonances is performed in the dielectron invariant mass range of 150-1,000 GeV/c^2 with an unbinned likelihood ratio statistics which is to be described in Sec. IV A. The upper limits on $\sigma \cdot \Gamma(X \to ee)$ at 95% C.L. are set as a function of mass, where the Xs are spin-1 or spin-2 particles and the mass limits with the SM coupling Z', E_6 Z's and the RS gravitons are also set, which are to be shown in Sec. IV B.

A. Resonances Search

The dielectron resonances search in the high-mass range of 150-1,000 GeV/c^2 is performed with an unbinned likelihood ratio, λ shown in Eq. 1

$$\begin{aligned}
\lambda &= \frac{\underset{n_b \geq 0}{max.}\mathcal{L}_b}{\underset{n_b \geq 0, n_s \geq 0}{max.}\mathcal{L}_{s+b}}, \quad 0 \leq \lambda \leq 1, \quad 0 \leq -2log\lambda \leq \infty \\
\mathcal{L}_{s+b} &= G_b \cdot \frac{(n_s+n_b)^N e^{-(n_s+n_b)}}{N!} \prod_i^N \frac{n_s S(x_i|\mu) + n_b B(x_i)}{n_s+n_b} \\
\mathcal{L}_b &= G_b \cdot \frac{n_b^N e^{-n_b}}{N!} \prod_i^N B(x_i) \\
G_b &= \frac{e^{-\frac{1}{2}(\frac{n_b-\bar{n}_b}{\sigma_b})^2}}{\frac{1}{2}[1+erf(\frac{n_b}{\sqrt{2}\sigma_b})]\sqrt{2\pi}\sigma_b}
\end{aligned} \tag{1}$$

, where the $\mathcal{L}_b$ is the likelihood for a null hypothesis which is described by the SM only, the $\mathcal{L}_{s+b}$ is that for a test hypothesis which is described by beyond SM together with the SM and the G_b is a background constraint. The n_s and n_b are unknown parameters and N is observed data, $\{x_i\}$. The $S(x|\mu)$ is a signal probability density function (PDF) which is a gaussian with a unknown mean (μ) and a known width and the $B(x)$ is a background PDF. The widths of the signal PDF are fixed to be compatible with the detector resolutions obtained from CDF simulation but the masses of the signal PDF are floated when we maximize the likelihood since we are searching for unknown resonances. Usually -2$log\lambda$ is widely used rather than λ itself. The details of the method are described in [11]. The -2$log\lambda$s are calculated as a function of mass in the search range of 150-1,000 GeV/c^2 with 1 GeV/c^2 step and it is shown in the left plot of Fig. 2. The most significant deviation between data and the SM prediction, which is the maximum $-2log\lambda$ is 14.38 at 241.3 GeV/c^2. The S/σ_B[16] corresponding to the region of maximum -2$log\lambda$ is calculated by counting the number of observed events and estimated backgrounds and it is 3.8.

To estimate the probability of observing an excess equal to or greater than the maximum observed excess anywhere in the search range of 150-1,000 GeV/c^2, we run 100,000 background only pseudo-experiments. The maximum -2$log\lambda$ anywhere in the search range is recorded in each pseudo-experiment. The right plot of Fig. 2 shows the maximum -2$log\lambda$ distribution recorded out of 100,000 background only pseudo-experiments. Even though we use 1 GeV/c^2 step size to scan -2$log\lambda$ through the search range, the maximum -2$log\lambda$ distribution in Fig. 2 is independent of the step size with a floating mass in maximizing the likelihood [11]. The probability of observing an equal or greater excess anywhere in the 150-1,000 GeV/c^2 mass range is defined as the fraction of pseudo-experiments with an equal or greater maximum -2$log\lambda$ than that shown in real data, which is 14.38 in this analysis and it is found to be 0.6%.

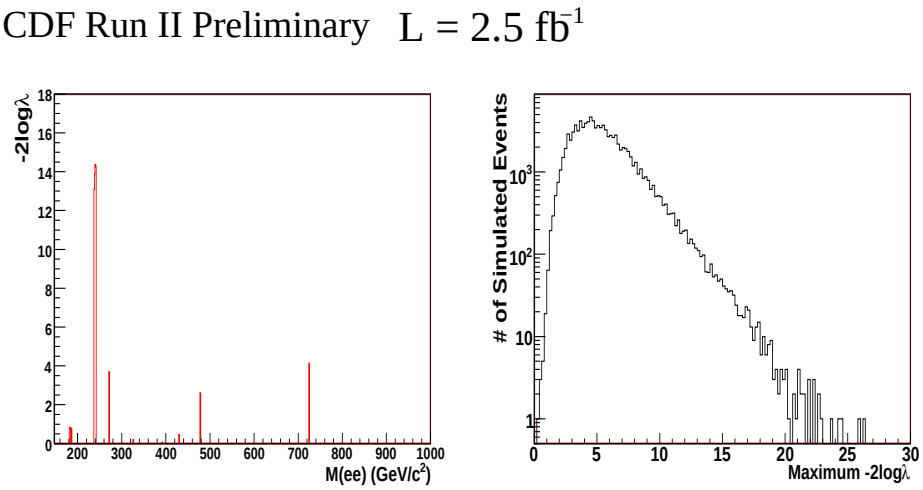

FIG. 2: The left plot is -2$log\lambda$ distribution based on 2.5 fb^{-1} of integrated luminosity and the right plot is the maximum -2$log\lambda$ distribution out of 100,000 background only pseudo-experiments.

B. Limits

The upper limits on $\sigma \cdot \Gamma(X \rightarrow ee)$ at 95% C.L. are calculated as a function of mass, where the Xs are spin-1 or spin-2 particles with a Bayesian binned likelihood method, of which details are described in [12]. The likelihood is a function of the signal cross section and is given by the Poisson. In order to allow for the uncertainty on the signal cross section due to the total efficiency and the background estimation uncertainties, the likelihood is convoluted with a gamma prior probability density. Then the posterior probability density function is formed with a constant prior for the signal cross section together with the likelihood. The limits are now obtained by integrating the posterior probability density function for the signal cross section until we achieve the required fraction (95% for this analysis) of the total integral from zero to infinity. Fig. 3 shows the observed upper limits from data and the expected one from background only pseudo-experiments for spin-1 particles as a function of dielectron invariant mass together with the cross section lines of Z's and Fig. 4 does the same for spin-2 particles together with the cross section lines of RS gravitons. The cross section lines for Z's and RS gravitons are calculated with the PYTHIA event generator. We use the couplings described in [13] for the Z's lines. A k-factor of 1.3 is multiplied to the PYTHIA calculation in order to show next-to-leading order cross sections. Table I shows the lower mass limits of the SM coupling and E_6 model Z's and Fig. 5 shows the excluded RS graviton mass region with respect to the $k/\overline{M}_{Pl}$.

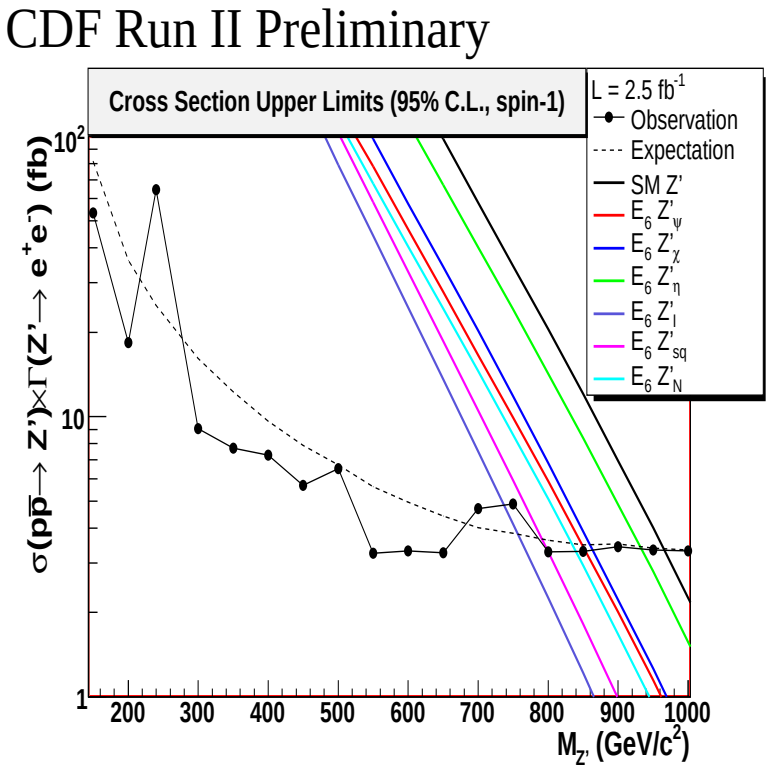

FIG. 3: The upper limits on $\sigma \cdot \Gamma(X \rightarrow ee)$ at 95% C.L., where the Xs are spin-1 particles.

Z' Model	Z'_{SM}	Z'_{ψ}	Z'_{χ}	Z'_{η}	Z'_{I}	Z'_{sq}	Z'_{N}
Exp. Limit (GeV/c^2)	965	849	860	932	757	791	834
Obs. Limit (GeV/c^2)	966	853	864	933	737	800	840

TABLE I: Observed and expected 95% C.L. lower limits on Z's masses.

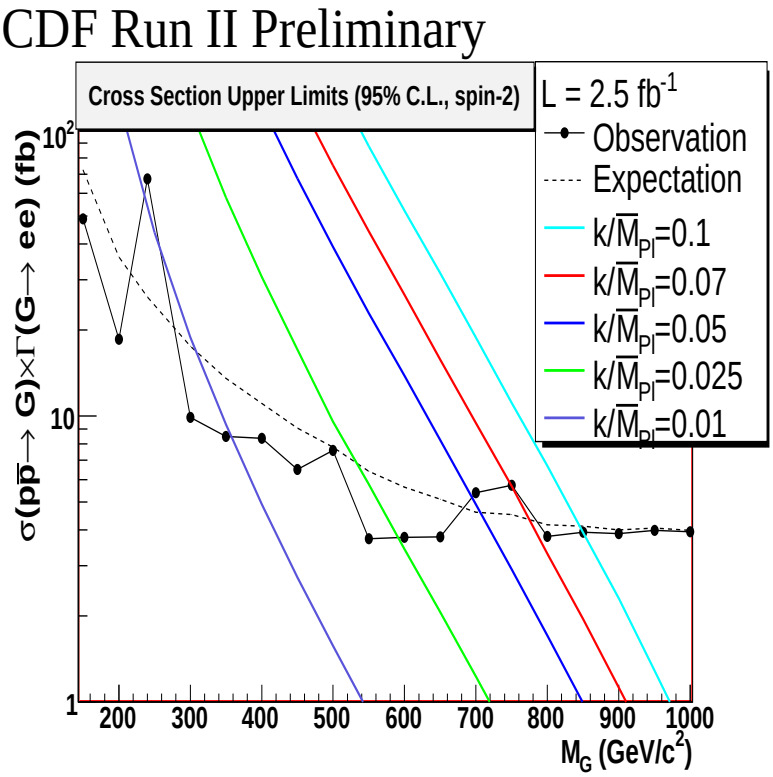

FIG. 4: The upper limits on $\sigma \cdot \Gamma(X \to ee)$ at 95% C.L., where the Xs are spin-2 particles.

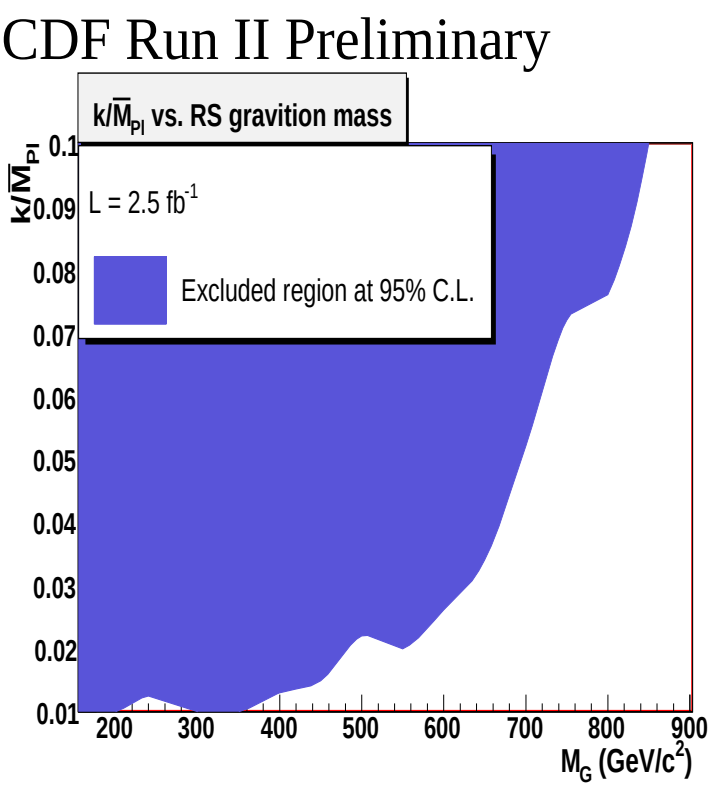

FIG. 5: The excluded RS graviton mass region with respect to the $k/\overline{M}_{Pl}$.

V. SYSTEMATIC UNCERTAINTIES

The dominant sources of systematic uncertainty in this analysis are the DY prediction, fake rate, luminosity and theoretical cross sections of other SM processes. Other systematic sources are the uncertainty on the scale factor of electron identification efficiency which comes from inconsistency between data and simulation (1.3% for CC and 2.3% for CP events), the energy scale (1.0% for both CC and CP events) and the energy resolution (0.6% for CC and 0.3% for CP events). The uncertainty related to the choice of the parton distribution functions set (CTEQ6M) [14] is evaluated using the Hessian method [15] and found to be 1.9% for CC and 0.6% for CP events.

VI. SUMMARY

We have searched for dielectron resonances with 2.5 fb^{-1} of CDF Run II data. The discrepancy between data and the expected background in the region of maximum excess of data over background is 3.8 standard deviations in the 240 GeV/c^2 region. This excess has a 0.6% probability that it is caused by the background fluctuation, given that the search probes the mass range 150-1,000 GeV/c^2.

The upper limits on $\sigma \cdot \Gamma$ at 95% C.L. are set for spin-1 and spin-2 particles. The SM coupling Z' with mass below 966 GeV/c^2 and the E_6 Z's with masses below 737/933 (lightest/heaviest) GeV/c^2 are excluded at 95% confidence level. The RS graviton with mass below 850 GeV/c^2 is excluded at 95% C.L. with $k/\overline{M}_{Pl} = 0.1$.

Acknowledgments

We thank the Fermilab staff and the technical staffs of the participating institutions for their vital contributions. This work was supported by the U.S. Department of Energy and National Science Foundation; the Italian Istituto Nazionale di Fisica Nucleare; the Ministry of Education, Culture, Sports, Science and Technology of Japan; the Natural Sciences and Engineering Research Council of Canada; the National Science Council of the Republic of China; the Swiss National Science Foundation; the A.P. Sloan Foundation; the Bundesministerium fuer Bildung und Forschung, Germany; the Korean Science and Engineering Foundation and the Korean Research Foundation; the Particle Physics and Astronomy Research Council and the Royal Society, UK; the Russian Foundation for Basic Research; the Comision Interministerial de Ciencia y Tecnologia, Spain; and in part by the European Community's Human Potential Programme under contract HPRN-CT-20002, Probe for New Physics.

---

[1] J. L. Hewett and T. G. Rizzo, Phys. Rept. **183**, 193 (1989).
D. London and J. L. Rosner, Phys. Rev. D. **34**, 1530 (1986).
[2] L. Randall and R. Sundrum, Phys. Rev. Lett. **83**, 3370 (1999).
[3] H. Davoudiasl, J. L. Hewett and T. G. Rizzo, Phys. Rev. Lett. **84**, 2080 (2000).
B. C. Allanach *et al.*, J. High Energy Phys. 12 (2002) 039.
[4] T. Aaltonen *et al.*, The CDF Collaboration, Phys. Rev. Lett. **99**, 171802 (2007).
[5] F. Abe *et al.*, Nucl. Instrum. Methods Phys. Res. A **271**, 387 (1988).
D. Amidei *et al.*, Nucl. Instrum. Methods Phys. Res. A **350**, 73 (1994).
F. Abe *et al.*, Phys. Rev. D **52**, 4784 (1995).
P. Azzi *et al.*, Nucl. Instrum. Methods Phys. Res. A **360**, 137 (1995).
The CDFII Detector Technical Design Report, Fermilab-Pub-96/390-E.
[6] C. Issever, AIP Conf. Proc. **670**, 371 (2003).
[7] T. Sjöstrand *et al.*, Comput. Phys. Commun. **135**, 238 (2001).
[8] Hamberg *et al.* (available at http://www.lorentz.leidenuniv.nl/~neerven).
[9] U. Baur and E. L. Berger, Phys. Rev. D **41**, 1476 (1990).
[10] S. Klimenko, J. Konigsberg, and T. M. Liss, FERMILAB-FN-0741 (2003).
[11] L. Demortier, "P values and nuisance parameters," to appear in the proceedings of the PhyStat-LHC Workshop on Statistical Issues for LHC Physics, CERN, Geneva, June 27-29, (2007).
Y. Gao *et al.*, Eur. Phys. J. C **45** 659-667 (2006).
[12] J. Heinrich *et al.*, physics/0409129 (2004).
[13] C. Ciobanu *et al.*, Fermilab, Report No. FERMILAB-FN-0773-E, (2005).
[14] H. Lai *et al.*, Phys. Rev. D **51**, 4763 (1995).
J. Pumplin *et al.*, J. High Energy Phys. **07**, 012 (2002).
[15] J. Pumplin *et al.*, Phys. Rev. D **65**, 014013 (2002).

[16] S is the number of signal and σ_B is $\sqrt{N_B + \sigma_{sys}^2}$, where N_B is the number of expected background and σ_{sys} is the systematic uncertainty of the N_B.